Thermal-gradient-induced interaction energy ramp and actuation of relative axial motion in short-sleeved double-walled carbon nanotubes



2011 Nanotechnology 22 485702

(http://iopscience.iop.org/0957-4484/22/48/485702)

Nanotechnology **22** (2011) 485702 (6pp) doi:10.1088/0957-4484/22/48/485702

# Thermal-gradient-induced interaction energy ramp and actuation of relative axial motion in short-sleeved double-walled carbon nanotubes

**Prathamesh M Shenai[1], Zhiping Xu[2] and Yang Zhao[1]**

[1] School of Materials Science and Engineering, Nanyang Technological University, 639789, Singapore
[2] Computational Energetics Laboratory, Department of Engineering Mechanics and Center for Nano and Micro Mechanics, Tsinghua University, Beijing 100084, People's Republic of China

E-mail: YZhao@ntu.edu.sg

Received 1 August 2011, in final form 25 September 2011
Published 4 November 2011
Online at stacks.iop.org/Nano/22/485702

**Abstract**
We investigate the phenomenon of actuation of relative linear motion in double-walled carbon nanotubes (DWNTs) resulting from a temperature gradient. Molecular dynamics simulations of DWNTs with short outer tube reveal that the outer tube is driven towards the cold end of the long inner tube. It is also found that the terminal velocity of the sleeve roughly depends linearly on the applied thermal gradient. We calculate the inter-tube interaction energy surface which is revealed to have a gradient depending upon the applied thermal gradient. Consequently, it is proposed that the origin of the thermophoretic motion of the outer tube may be attributed partially to the existence of such an energy gradient. A simple analytical model is presented accounting for the gradient in energy profile as well as the effect of biased thermal noise. It is shown that the proposed model predicts the dynamical behaviour of the long-time performance reasonably well.

(Some figures may appear in colour only in the online journal)

## 1. Introduction

The last decade in nanoresearch saw a significant focus on carbon nanotubes (CNTs) with respect to putting them in practical applications ranging from nanoelectronics [1] and nanomechanical devices [2–4], to space elevators [5, 6]. A new field being opened to vast possibilities by the virtue of the supreme mechanical properties of CNTs is nanomechanics. A plethora of prospective nanodevices that could be built from CNTs including oscillators, bearings, resonators, springs and mass sensors is only limited by technological challenges such as precision manufacturing, control and accurate drive mechanisms [2–4]. Molecular dynamics (MD)-based studies have been employed quite successfully as a convenient pathway for studying nanodevices, which has uncovered various interesting physical aspects [7–10].

Recent experiments suggest that application of a thermal gradient can possibly provide control over the direction and speed of relative axial motion in multi-walled carbon nanotubes (MWNTs) [4, 11]. Yet, the mechanism behind temperature-gradient-actuated motion has not acquired a concrete theoretical footing. The motion characteristics bear similarities with 'thermophoresis'—a phenomenon commonly encountered in gaseous mixtures or colloids subjected to a spatial thermal gradient [12, 13]. Although satisfactorily studied in the case of gases, mechanisms behind thermophoresis in liquid media are surrounded by contention. The relative motion in an MWNT resulting from spatial temperature difference is even more complicated. In the simplest terms, it can be viewed as the movement of a solid over another solid surface subjected to a thermal gradient. As a result any direct extension from theories legitimately operating in gas-like or liquid-like regimes is difficult.

Prior to the first experimental evidence that temperature differences can be used to drive nanoscale motion in CNTs [4],

 

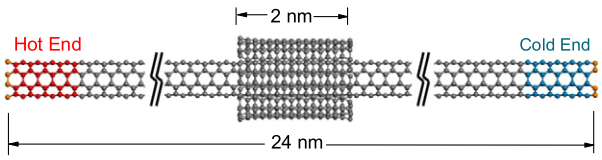


**Figure 1.** Schematic of the (4, 4)/(9, 9) model DWNT used to study thermally driven motion. Edge atoms at both ends (in orange colour) are fixed in position, while red and blue coloured regions are thermostated at relatively high and low temperatures, respectively.

Ou-Yang *et al* had hypothesized the possibility of achieving directional control in DWNTs subjected to time-varying temperature [14] as well as time-varying voltage applied along the axial direction [15]. In an MD study of gold nanoclusters (NP) enclosed in long SWNTs, Schoen *et al* [16] uncovered the signature thermophoretic motion of the NP, arguably noted for the first time in the case of solid–solid interfaces. Under the influence of thermophoretic force, the NP moves towards the cold end with the specifics of its linear and rotational motion dictated by the nanotube chirality. The excitation of radial-breathing-like phonon modes was eventually found essential in actuating the NP to the cold end [17]. A few other MD studies revealed that water can also be transported across CNTs subjected to the axial thermal gradient as small as 1.05 K nm$^{-1}$ [18, 19]. Interestingly, it was found that the average potential energy of interaction between water–water or water–CNT increases linearly with the applied gradient. Irrespective of the encaged species, it was found that its mean terminal velocity linearly increases with thermal gradient. An ambiguity is present in the literature since some researchers find a linear dependence of thermophoretic velocity on thermal gradient while others argue for a linearly dependent thermophoretic force.

In their study of DWNT systems, Zambrano *et al* found a short inner tube moving under the influence of a temperature gradient in excess of 1.18 K nm$^{-1}$ [20]. Their results, however, exhibit large fluctuations in force calculations while the choice of DWNT configuration with inter-tube distance much greater (3.9 Å) than the equilibrium distance (3.4 Å) in DWNTs appears somewhat unconventional. Hou *et al* considered a short outer tube mounted on a long inner tube configuration and estimated the thermal driving force to be of the order of piconewtons [21]. Along with the typical linear dependence of the thermal force on the gradient, its relative indifference to the average system temperature was also put forth. A qualitative argument is usually raised that the phonon current being set up in the inner tube may collide and transfer some momentum to the outer tube [4, 21]. Combined with their finding that the thermophoretic force is relatively independent of the tube length (when greater than 5 nm), it is proposed that the radial-breathing modes (RBM) play a major role and interaction with the edge atoms are important. Even though the contribution from RBM is believed to be most important, direct evidence has not been observed yet in the case of DWNTs. While other MD studies dealing with DWNT [22] or SWNT-C60 [23] systems also find features characteristic of thermally driven diffusion, the question of the origins of the effective driving force stays open.

The current work attempts to probe in detail the origins of the effective driving force in DWNT systems subjected to thermal gradient. In section 2, details of the MD simulations are enlisted. Simulation results are presented and discussed in section 3. Analysis of the actuation of motion by a thermal gradient is delineated in section 4 and a very simple analytical model is also proposed in section 5. Finally, conclusions are drawn in section 6.

## 2. Methodology

We use MD simulations to investigate the induction of relative inter-tube motion in DWNTs as a result of an applied thermal gradient. The DWNT configuration used consists of a 24 nm long inner (4, 4) SWNT and a 2 nm long outer (9, 9) SWNT as shown in figure 1. The adaptive intermolecular reactive empirical bond order (AIREBO) potential is used to describe the C–C intramolecular and intermolecular interactions [24]. Geometry optimization is carried out with a conjugate-gradient algorithm. An MD package LAMMPS is used to perform dynamics calculations with a velocity-Verlet integration scheme [25]. For all the simulations, a timestep of 1 fs is employed. In the initial configuration, both tubes share the same centre of mass. To maintain spatial orientation, all the edge atoms at each end of the (4, 4) SWNT are fixed in position.

The MD simulations are carried out in three steps. The first step consists of isothermal equilibration in which both the inner and outer CNTs are thermalized at 300 K. Thermalization is carried out by performing MD simulations in a canonical ensemble (constant *NVT*) for 100 ps using a Berendsen thermostat [26]. The next stage consists of performing non-equilibrium MD in order to establish a steady temperature gradient along the length of the inner tube. A region of about 1 nm length (excluding the fixed atoms) at each end of the inner tube is used for temperature control by the Berendsen thermostat. One end of the inner tube is thus maintained at 300 K, while the other is at a high temperature (400, 500, 600, 700 and 800 K). No temperature control is exercised over the rest of the atoms, which are subjected to *NVE* conditions. To achieve a steady thermal gradient across the length of the inner tube, this stage is carried out for 1030 ps. During the initial 30 ps of this period, the edge atoms at each end are fixed only in $x$ and $y$ directions ($z$ axis being along the length of the tubes) to lower any unwanted strain in the inner tube. During this period, the centre of mass of the outer tube is constrained. At the end of the second step, the restriction on the outer tube's centre of mass is removed. This final step is the actual production run, which is carried out for another 1 ns.

## 3. Results and discussions

Using the aforementioned scheme, we performed non-equilibrium MD simulations on the (4, 4)/(9, 9) configuration subjected to different thermal gradients of 4.5, 9, 13.5, 18 and 22.5 K nm$^{-1}$ along the inner tube. Figure 2(a) shows the $z$ coordinate of the centre of mass of the outer tube as a function of time, for various thermal gradients. Each curve in this

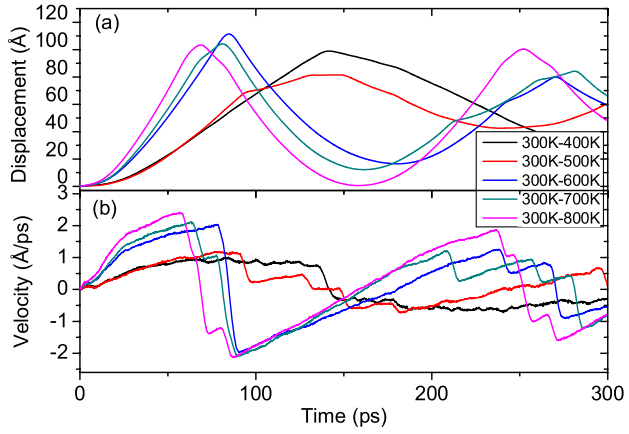


**Figure 2.** (a) Displacement and (b) velocity of the centre of mass of the outer (9, 9) tube as a result of different thermal gradients applied across the inner (4, 4) nanotube.

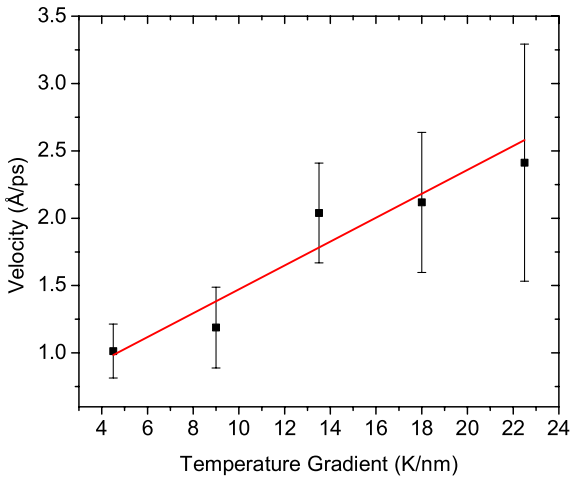


**Figure 3.** Averaged terminal velocity of the outer tube as a function of different thermal gradients of 4.5, 9, 13.5, 18 and 22.5 K nm$^{-1}$.

plot is obtained after averaging over four different trajectories. It is clear that, in each case, the mobile tube starts to move against the thermal gradient. It accrues momentum as it travels towards the cold end and gets reflected back by the repulsive potential barrier. The bounced-back motion is opposed by the 'force' of the imposed thermal gradient. As a result, the outer tube halts briefly at a point where the two opposing forces balance each other before resuming towards the cold end under the imposed temperature difference. Figure 2(b) shows the corresponding velocity ($z$ component) of the centre of mass of the mobile tube. The slowdown as the tube approaches the cold end and a sharp bounce back resulting in velocity reversal are apparent. It can be noted that the maximum (or terminal) velocity attained by the outer tube increases as the thermal gradient becomes larger since the thermophoretic force acting on the particles increases with the thermal gradient. In figure 3, maximum velocity attained by the outer tube is plotted against the different thermal gradient. The terminal velocity increasing in a roughly linear manner with the gradient can be observed, highlighting the nature of the motion to be thermophoretic. To ensure the directional control it is also verified that the motion gets reversed if the thermal gradient is reversed.

For a short period of 30 ps during the simulation run, thermal expansion/contraction is allowed in the axial direction. However, the tube may exhibit a radial response to the temperature gradient as well. Figures 4(a) and (b), respectively, shows the temperature profile and the change in the local radius of the (4, 4) nanotube along its length. The profile of temperature gradient shows non-Fourier conduction behaviour, typically observed in carbon nanotubes. From figure 4(b), it further appears that the inner tube has a slightly engorged radius near the hot end as compared to that at the cold end. Although the change in radius is very small (0.006 Å), a non-zero gradient in the radius can still be observed. As the inter-tube interaction energy depends significantly on the inter-tube radius, such a trend could indicate possible energetic difference for motion of the outer tube in different axial directions. It should be noted, however, that the change in radii is smaller than the typical amplitude of thermal vibrations of atoms

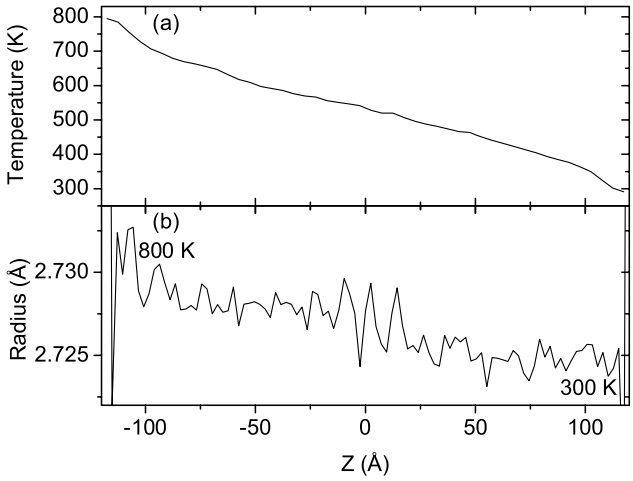


**Figure 4.** Variation of the (a) temperature and (b) local radius of the inner tube along its length. The hot and cold ends (left and right, respectively) are maintained at 800 and 300 K, respectively.

for the applied temperature range. Nevertheless, the inner tube experiences significant deformations which can likely affect the motion of the outer tube. As a result, when the outer tube is allowed to move, it may be expected that the tube travels towards the lower temperature end favoured by energetic considerations. Long simulation runs (5 ns) show that, in general, the outer tube does not completely stop near the cold end, but oscillates with a small amplitude of about 10 Å. However, in some instances it is also possible for the outer tube to traverse to an increased oscillation amplitude as well.

MD results from the current work and previous literature reports suggest that a small mobile element in a thermally graded system involving carbon nanotubes moves towards the cold end. However, unlike the comparatively well-studied gaseous systems or colloidal systems, exhibition of thermophoretic motion in the current context is in a nanoscale system. It is more accurate to say that this is a solid–solid interfacial phenomenon. The origins of the thermophoretic

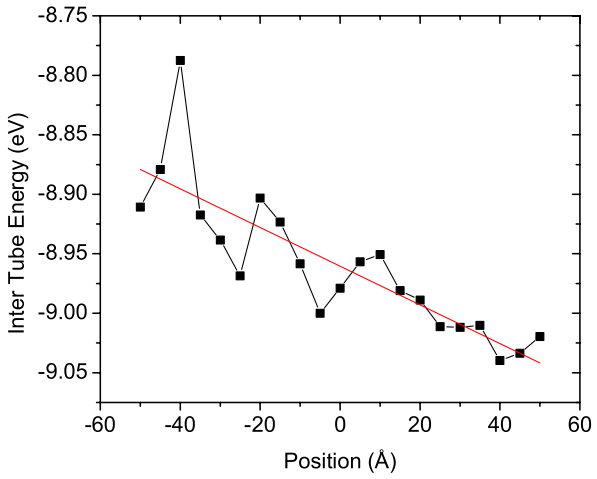


**Figure 5.** Variation of inter-tube van der Waals energy with different initial positions of the outer tube in the (4, 4)/(9, 9) DWNT configuration. The hot and cold ends of the inner tube are maintained at 800 K and 300 K, respectively.

force even in the colloidal systems are heavily debated. Different theories have been proposed which pursue the origins of effective force using the approach of either hydrodynamics or energetics [13]. Simply speaking, a net bias in the collision-induced impulse on a particle suspended in a liquid subjected to thermal gradient results in directionality in its motion. Recent *in situ* observation of trapped nanoparticles inside MWNTs which are subjected to temperature differences indicate that the thermal diffusion of the particles is stochastic [11].

## 4. Interaction energy gradient induced by temperature difference

Despite substantial efforts, satisfactory fundamental reasoning behind the existence of the 'effective' thermal force in nanotube systems has not emerged and is sought after in the present work. As revealed from the MD simulations, even after a long period is used to establish a steady thermal gradient across the inner tube, the outer tube stays at a relatively uniform temperature owing to its small size. In qualitative terms, in the region where the outer tube is located, the inner tube atoms at a hotter region will undergo a larger-amplitude random displacement in the radial direction as compared to those at the colder region. Further, the interaction energy between the two tubes depends upon the average inter-tube distance. It is then easy to visualize that the inter-tube van der Waals energy will vary depending upon the position of the outer tube, and that the temperature gradient may induce a gradient in the inter-tube interaction energy when viewed as a function of the position of the outer tube. A straightforward quantification could be obtained by calculating the inter-tube energy profile after rigid-body translation of the outer tube in small increments. However, this approach is met with a few operational challenges. The inner tube undergoes significant wavy deformations during the temperature gradient set-up phase of the simulations. This presents difficulties in obtaining the desired energy profile as the rigid-body translation of the outer tube can result in unmatched form factors of the two tubes. Hence we chose to follow an indirect approach described below to obtain the energy profile.

An initial structure of the DWNT is prepared in such as way that the outer tube has a desired $z$ coordinate ($z$) for its centre of mass. The methodology described in the final paragraph of section 2 is carried out (with the hot end at 800 K and cold end at 300 K) for different values of $z$ from $-50$ to 50 Å with an increment of 5 Å. The 100 ps data just before the production run (i.e. allowing the outer tube to move) is used to calculate the average inter-tube van der Waals energy. The resultant inter-tube interaction energy plot against the position of the outer tube is shown in figure 5. It can be observed that, even though the variations are large, a gradient in the inter-tube energy is present. A linear fit reveals the energy gradient to be 0.0162 eV nm$^{-1}$. Hence, the interaction energy is higher when the outer tube is towards the comparatively hotter end. Such a gradient is manifested as a 'thermal force' acting on the outer tube. For the temperature gradient of 22.5 K nm$^{-1}$, an order-of-magnitude estimation for the thermal force is 2.7 pN.

An estimation of the total force acting on the outer tube can be obtained from the MD data by assuming that its velocity varies linearly during the period when it moves from the centre towards the cold end. Using such an approximation for the MD data from 300 to 800 K gradient simulation, we estimate the total force acting on the outer tube to be 13.8 pN. In comparison, the maximum 'thermal force' that can be extracted from our hypothesized energy gradient is 2.7 pN. The apparent discrepancy is expected due to the adopted methodology and the approximate nature of our order-of-magnitude estimation for the thermal force. During the production MD run the outer tube undergoes translation and its temperature is not in equilibrium with the local temperature of the inner tube due to the short time of contact. On the other hand, the energy profile of figure 5 is obtained from the equilibration period of the simulations. Hence, the correlation between instantaneous energy profile during the actual production MD run with that reflected by figure 5 will be complex. It is also possible that other mechanisms originating from entropic considerations or free energy reduction could provide an additional driving force independent of the mechanism we propose in this paper. Additionally, the origin of the thermal force does not account for other deforming modes such as wavy modes that stay strongly evident in the MD results. The excitation of wavy modes has been reported in a number of studies, especially concerning the energy dissipation in nanotube devices [8, 27]. It is possible that a part of the energy contained in such modes gets channelled into the axial motion of the outer tube. It was shown previously that the presence of radial-breathing modes is necessary to drive the cargo in nanotube–Au cluster systems. However, no quantification for its effect on displacement or velocity is known.

## 5. Motion in a titled periodic potential

Even in isothermal simulations, Xu *et al* demonstrated that a short mobile tube can undergo large amplitude axial or rotational motions governed by the interaction energy surface

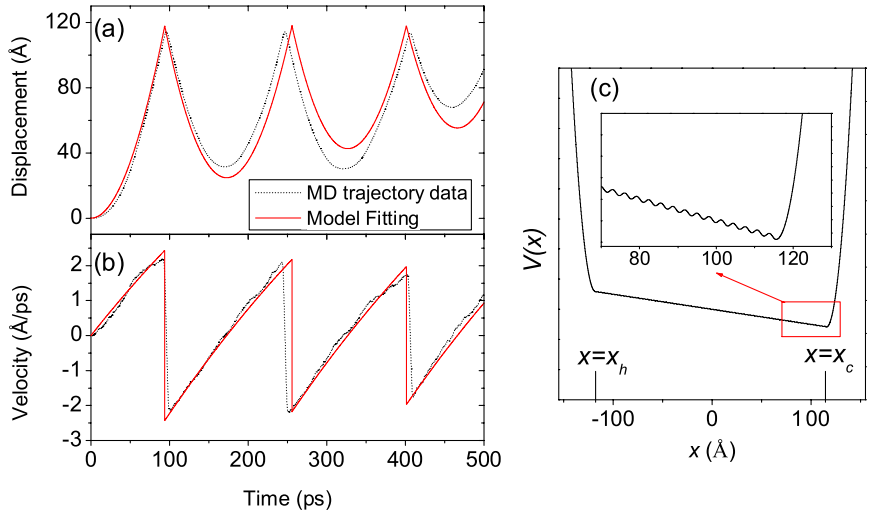


**Figure 6.** Based on the 1D tilted potential model as described in the text, (a) displacement and (b) corresponding velocity curves with time. The important fitting parameters used are $b = 0.0162$ eV nm$^{-1}$, $\gamma = 6.775$ amu ps$^{-1}$, $\langle \xi(t) \rangle = 14.35$ pN and amplitude of the noise fluctuations is 28.7 pN. (c) A schematic of the 1D potential model described in the text is shown. The inset shows a magnified region corresponding to the outer tube reaching the end of the inner tube.

between the tubes [28]. However, the thermally excited motion cannot be rectified without any external impulse. In the current context, directionality is achieved by the use of bias in thermal energy. In a long inner tube with a temperature gradient set-up, along its length the phonon occupation is expected to be different. Although a stochastic model is more appropriate to describe the thermal-gradient-induced motion for simplicity, we chose a kinetic model. The outer tube can be treated as a large particle moving under the influence of a titled potential, whose presence is found via MD simulations. The 'thermophoretic driving force' is then the gradient of the potential energy ($F_{\rm th} = -\frac{{\rm d}V(x)}{{\rm d}x}$). The equation of one-dimensional (1D) motion for a particle of mass $m$ can then be written as

$$m\frac{{\rm d}^2x}{{\rm d}t^2} = F_{\rm th} + F_{\rm fri} + \xi(t) \tag{1}$$

where $F_{\rm fri}$ is the frictional force and $\xi(t)$ is the thermal noise (ideally, $\langle \xi(t) \rangle = 0$). As the velocity of the outer tube is observed to be comparatively small, frictional force is considered proportional to the velocity as $F_{\rm fri} = -\gamma \frac{{\rm d}x}{{\rm d}t}$.

The above equation of motion can be easily solved for constant $F_{\rm th}$ to yield exponential expressions for both the velocity and the displacement if $\xi(t)$ is disregarded. However, consideration of the noise term can be expected to be important due to the relatively high temperatures at which simulations in this work are carried out. We thus chose to solve the equation of motion numerically, wherein the integration is performed with a Verlet velocity algorithm. The potential form shown schematically in figure 6(c) is approximated as

$$V(x) = \begin{cases} a\sin(f(x - x_{\rm c})) - b(x - x_{\rm c}) & x_{\rm h} \leqslant x \leqslant x_{\rm c} \\ (x - x_{\rm c})^2/d & x > x_{\rm c} \\ V(x_{\rm h}) + (x_{\rm h} - x)^2/d & x < x_{\rm h} \end{cases} \tag{2}$$

where $a$, $b$, $f$ and $d$ are the parameters chosen suitably while $x_{\rm c}$ and $x_{\rm h}$ respectively represent distance of the cold and hot ends of the inner tube from the midpoint. For $x_{\rm h} \leqslant x \leqslant x_{\rm c}$, the potential form is a sinusoidal function slanted at a slope of $b$, which is extracted from the linear fit to the interaction energy profile shown in figure 5. For $x > x_{\rm c}$ and $x < x_{\rm h}$, matching parabolas are chosen so as to model the repulsive potential barrier at the end of a DWNT.

Figures 6(a) and (b) show the displacement and the velocity of a particle moving in the 1D potential $V(x)$ fitted to the data from the MD simulations and with non-zero mean noise. The particle moves against the potential gradient and gets reflected back to a certain distance before traversing back against the gradient. The frictional force serves to dampen the oscillation while the thermal noise serves to modulate it. It is interesting that this simple model can qualitatively reproduce the displacement and velocity features observed in MD results. It should be noted that, since the 'effective thermal force' itself is of insufficient magnitude to drive the particle at the observed speed, the surplus required force has been accommodated in the form of non-zero mean of the noise. The surplus bias required to generate sufficient force might be argued to arise from other complicated factors such as differential phonon occupations in the inner tube on two sides of the outer tubes, or as a result of possible entropic or free energy reduction considerations.

Controllable actuation of relative motion along the axial direction is thus rendered viable by simply applying a temperature difference. Although we have used very large thermal gradients in this paper, similar to many other previous studies [4, 16, 22], the motion characteristics are well exhibited at much lower and experimentally accessible temperature gradients. In experiments, very long multi-walled CNTs with lengths as large as 1 $\mu$m are used. In contrast, MD simulations typically deal with thousands of atoms, and thus the fluctuation of temperature is much more enhanced in comparison to experimental conditions. Consequently, by using large gradients, fluctuations can be kept as low as possible and

essential features of thermally driven motion can be studied comparatively easily. Such a mass transport technique could be useful in various other configurations—such as encapsulated matter (e.g. fullerenes, metal nanoclusters, biomolecules) inside CNTs. It will also be possible to exercise a reversal of direction of motion by simply reversing the direction of the thermal gradient.

## 6. Conclusions

We have carried out MD simulations on (4, 4)/(9, 9) DWNT configurations with a short (9,9) tube and the long inner tube subjected to a thermal gradient. For various temperature gradients (from 4.5 to 22.5 K nm$^{-1}$), the sleeve is found to slide along the axial direction opposite to the thermal gradient. The terminal velocity of the outer tube depends roughly linearly upon the applied thermal gradient. We study the energy of inter-tube van der Waals interactions in the (4, 4)/(9, 9) DWNT, and it is found to possess a gradient due to the temperature difference across the ends of the inner tube. We propose that such a gradient in energy leads to a 'thermal force'. For a temperature gradient of 22.5 K nm$^{-1}$, the magnitude of the resulting average thermal force is found to be 2.7 pN. Although the proposed thermal force is insufficient in driving the outer tube to corroborate the MD results, it nevertheless stands as one of the acting mechanisms that contribute to the thermophoretic behaviour of the outer tube.

A simple 1D model is proposed that includes a thermal force resulting from the energy gradient and reproduces qualitative features of the motion of the outer tube well. Using the same model, it is argued that in the DWNT systems driven by thermal gradients, the thermal noise plays a very important role, and a bias in thermal noise is needed to quantitatively obtain the required magnitudes of the thermophoretic force. The nature of the thermally driven motion as a highly stochastic process is thus highlighted.

## Acknowledgments

Support from the Singapore National Research Foundation through the Competitive Research Programme (CRP) under project no. NRF-CRP5-2009-04 and the Singapore Ministry of Education through the Academic Research Fund (Tier 2) under project no. T207B1214 is gratefully acknowledged.

## References

[1] Lu W and Lieber C M 2007 *Nature Mater.* **6** 841
[2] Bourlon B, Glattli D C, Miko C, Forro L and Bachtold A 2004 *Nano Lett.* **4** 709
[3] Cumings J and Zettl A 2000 *Science* **289** 602
[4] Barreiro A, Rurali R, Hernández E R, Moser J, Pichler T, Forro L and Bachtold A 2008 *Science* **320** 775
[5] Xu Z, Wang L and Zheng Q 2008 *Small* **4** 733
[6] Yakobson B I and Smalley R E 1997 *Am. Sci.* **85** 324
[7] Zheng Q S and Jiang Q 2002 *Phys. Rev. Lett.* **88** 045503
[8] Zhao Y, Ma C C, Chen G H and Jiang Q 2003 *Phys. Rev. Lett.* **91** 175504
[9] Tangney P, Louie S G and Cohen M L 2004 *Phys. Rev. Lett.* **93** 065503
[10] Xu Z P, Zheng Q S, Jiang Q, Ma C C, Zhao Y, Chen G H, Gao H and Ren G X 2008 *Nanotechnology* **19** 255705
[11] Zhao J, Huang J Q, Wei F and Zhu J 2010 *Nano Lett.* **10** 4309
[12] Goldhirsch I and Ronis D 1983 *Phys. Rev.* A **27** 1616
[13] Piazza R 2008 *Soft Matter* **4** 1740
[14] Tu Z C and Ou-Yang Z C 2004 *J. Phys.: Condens. Matter* **16** 1287
[15] Tu Z C and Hu X 2005 *Phys. Rev.* B **72** 033404
[16] Schoen P A E, Walther J H, Arcidiacono A, Poulikakos D and Koumoutsakos P 2006 *Nano Lett.* **6** 1910
[17] Schoen P A E, Walther J H, Poulikakos D and Koumoutsakos P 2007 *Appl. Phys. Lett.* **90** 253116
[18] Zambrano H A, Walther J H, Koumoutsakos P and Sbalzarini I F 2009 *Nano Lett.* **9** 66
[19] Shiomi J and Maruyama S 2009 *Nanotechnology* **20** 055708
[20] Zambrano H A, Walther J H and Jaffe R L 2009 *J. Chem. Phys.* **131** 241104
[21] Hou Q W, Cao B Y and Guo Z Y 2009 *Nanotechnology* **20** 495503
[22] Coluci V R, Timóteo V S and Galvão D S 2009 *Appl. Phys. Lett.* **95** 253103
[23] Rurali R and Hernández E R 2010 *Chem. Phys. Lett.* **497** 62
[24] Stuart S J, Tutein A B and Harrison J A 2000 *J. Chem. Phys.* **112** 6472
[25] Plimpton S 1995 *J. Comput. Phys.* **117** 1
[26] Berendsen H J C, Postma J P M, van Gunsteren W F, DiNola A and Haak J R 1984 *J. Chem. Phys.* **81** 3684
[27] Shenai P M, Ye J and Zhao Y 2010 *Nanotechnology* **21** 495303
[28] Xu Z P, Zheng Q and Chen G 2007 *Phys. Rev.* B **75** 195445